13th World Conference on Earthquake Engineering
Vancouver, B.C., Canada
August 1-6, 2004
Paper No. 135

EFFECTS OF FRACTURE MATERIAL PROPERTIES ON CRACK PROPAGATION OF CONCRETE GRAVITY DAMS DURING LARGE EARTHQUAKES

Kenichi KANENAWA[1], Takashi SASAKI[2], Yoshikazu YAMAGUCHI, Dr. Eng.[3]

SUMMARY

In Japan, the earthquake-resistant design of dams is based on the seismic coefficient method. Many existing dams in Japan have experienced strong earthquake ground motions. However, no serious damage on these dams has been observed during large earthquakes including the Kobe Earthquake in 1995. So, it is judged that their seismic resistance is adequately high. But, after the Kobe Earthquake, it is desired to guarantee seismic resistance of dams against large earthquake motions. With progress in computer performance and numerical analysis technologies, to evaluate rationally the safety of dams during earthquakes is required by simulating of dynamic behaviors of dams more realistically. The crack generated in concrete dam body is considered as one major type of damage modes to concrete gravity dams during large earthquakes. We carried out the crack progress analysis for concrete gravity dam using the smeared crack model considering the tensile fracture of concrete. Here, we revealed the characteristics of effects of the tension-softening properties of concrete on the occurrence and the progress of cracks in a dam body.

1. INTRODUCTION

The crack in concrete dam body is considered as one major type of damage modes to concrete gravity dams during large earthquakes. The discrete model and the smeared crack model are major methods to consider the tensile fracture of concrete in the numerical analysis [1]. The discrete model is necessary to beforehand set the elements that can describe cracks in proper locations where cracks may occur. But the smeared crack model doesn't need to determine the

[1] Researcher, Dam Structure Research Team, Hydraulic Engineering Research Group, Public Works Research Institute (PWRI), JAPAN
[2] Senior Researcher, ditto
[3] Principal Researcher, ditto

locations where the crack may occur in advance. Because it is difficult to estimate such locations in the dam body, we have conducted researches on the crack progress analysis of the concrete gravity dam using the smeared crack model and the safety evaluation method during the earthquake [2]. Fracture progress of concrete material is generally considered to be governed by tension-softening properties of concrete material such as stress at the beginning of tension-softening, fracture energy and shape of tension-softening curve. Here, we report results of study on effects of the tension-softening properties of concrete on the occurrence and the progress of cracks in a dam body.

2. BEHAVIOR UNDER SINUSOIDAL WAVE

2.1 Analysis Conditions

Crack progress analyses for concrete gravity dams under sinusoidal waves were carried out by the smeared crack model to study the effect of the material properties related to the fracture of concrete on the occurrence and progress of cracks in dam bodies. The analysis models are concrete gravity dams with a dam height of 100m and 3 different shapes as shown in Figure 1. The material properties of concrete used for the analysis are summarized in Table 1. The damping was set as the Rayleigh type damping using the first and third natural frequencies for the linear model without considering crack occurrence. And the analyses were carried out using a tension-softening curve expressed by the single straight line shown in Figure 2. Self-weight and hydrostatic pressure were considered as static loads. The boundary condition of a bottom of a dam body was set as rigid and an effect of a reservoir was considered by a consistent added mass matrix obtained assuming water was incompressible fluid. The uplift pressure was not considered. We inputted the sinusoidal wave with acceleration amplitude of 150gal horizontally from the bottom of the dam body. The frequency of the sinusoidal wave is about the first natural frequency of dam. The input wave used for the analysis of Model-2 is shown in Figure 3, and the specifications of the input wave used for each dam are summarized in Table 2. The general-purpose finite element method analysis program "Diana" [3] was used for the analysis.

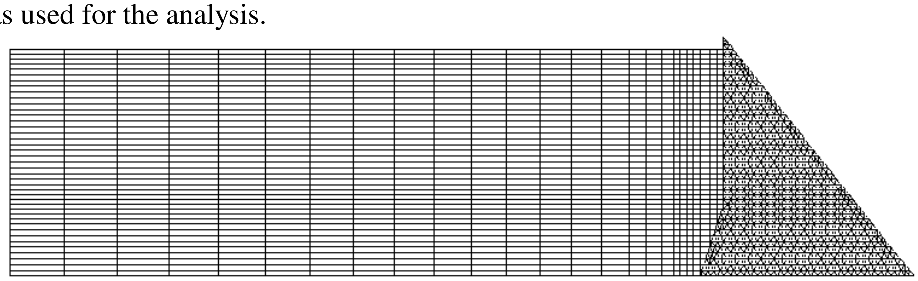

(a) Reservoir and Dam Body (Model-2)

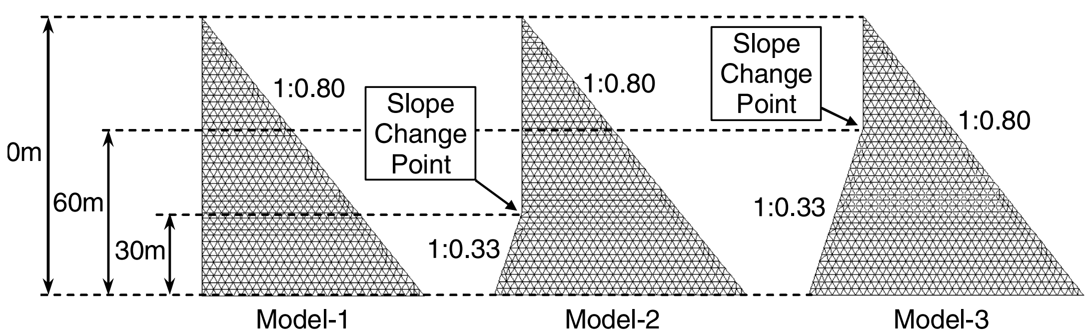

(b) Only Dam Body

Figure 1 FE-Model

Table 1 Material Properties of Concrete

Young's Modulus of Elasticity *E* (MPa)	3.00E+04
Poisson's Ratio *v*	0.2
Stress at Beginning of Tension-Softening *ft* (MPa)	2.0, 2.5, 3.0, 4.0
Fracture Energy *Gf* (N/m)	100, 200, 300, 400, 500
Compressive Strength *fc* (MPa)	*ft*×10
Unit Mass ρ (kg/m^3)	2,300
Damping Ratio *h* (%)	10 (Rayleigh damping, the first and third natural frequency)

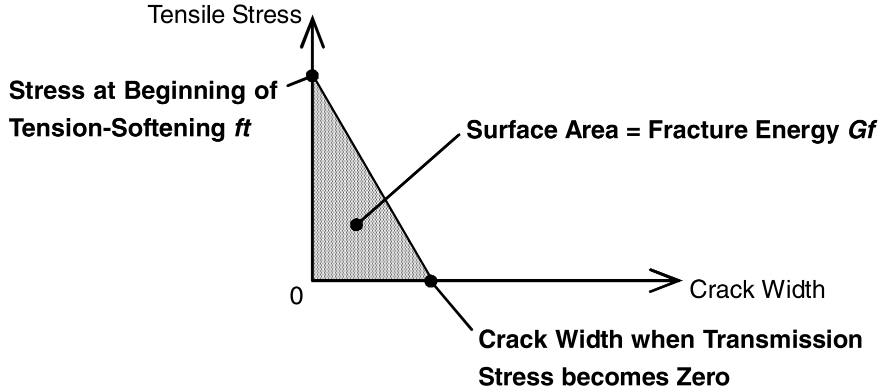

Figure 2 Tension-Softening Curve (Single Straight Line Approximation Model)

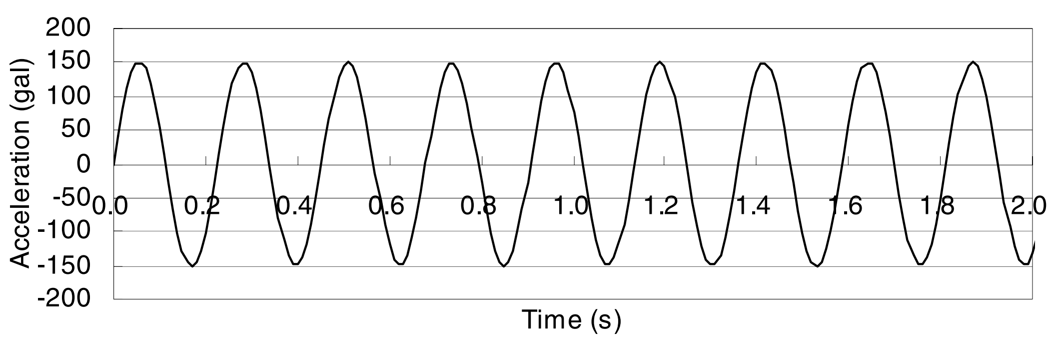

Figure 3 Input Wave for Model-2

Table 2 Specifications of Input Wave

Model #	Model-1	Model-2	Model-3
Frequency (Hz) (First Natural Frequency)	4.10	4.41	5.18
Period (s) (First Natural Period)	0.24	0.23	0.19
Acceleration Amplitude (gal)	150	150	150

2.2 Results of Analysis

2.2.1 Response of Dam Body

Figure 4 shows the time history of the acceleration response and the displacement response at the crest of dam in the linear dynamic analysis of Model-2. The downstream side is considered to be positive. The figure shows the response acceleration of more than 2,000 gal at the crest. As shown in Figure 4 (b), the time points when the crest was greatly displaced on the downstream side are called here the first wave and the second wave in sequence. The figure finds that the response of the dam body becomes almost constant at about the fourth or fifth wave.

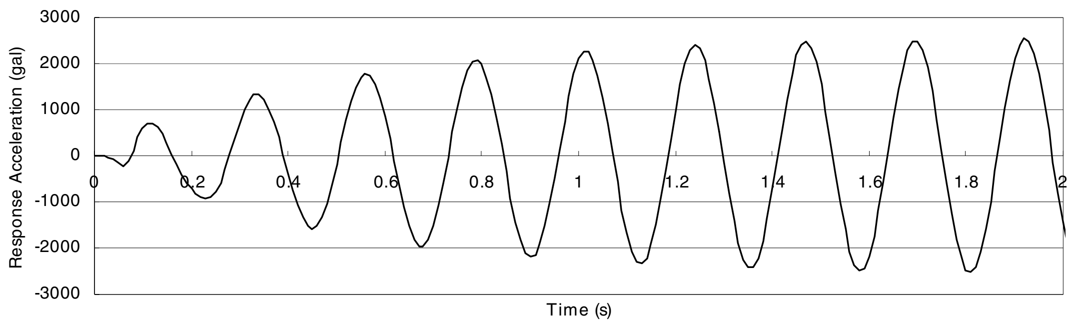

(a) Acceleration

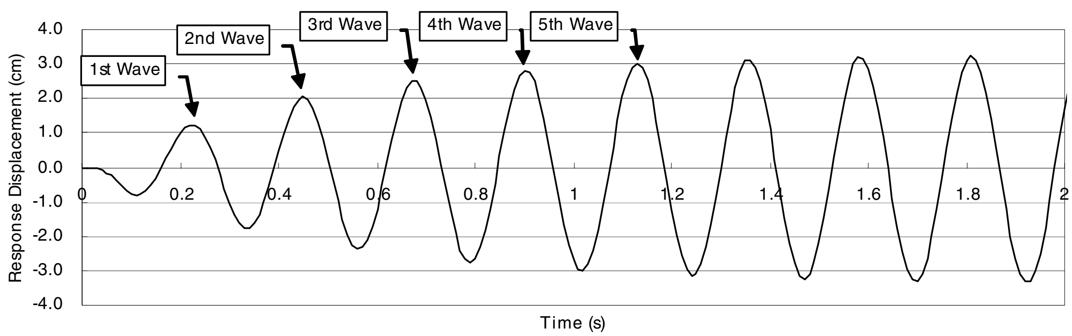

(b) Displacement
Figure 4 Response Time History of Crest

2.2.2 Location of Crack Occurrence during Earthquake

Figure 5 shows the location where cracks finally generated as the results of the crack progress analysis in the three models on the conditions that stress at beginning of tension-softening *ft* was 3.0 MPa and the fracture energy *Gf* was 300N/m. This shows the locations of all cracks that occurred throughout the analysis, and cracks occurred on the black colored elements. From this figure, it is seen that during an earthquake, cracks occur near the bottom of the dam body in Model-1, and near the changing point of the slope and the bottom in Model-2 and Model-3. Because the foundation was not included in this analysis model, the stress concentration occurred at the bottom of the body and the progress of the crack in such part is conspicuous. The cracks tend to occur in the bottom and near the slope change point during the earthquake. As shown in Figure 6, the cracks may also occur on the downstream of the dam body according to the size of the earthquake acceleration, the type of the seismic wave or the tensile strength of the concrete.

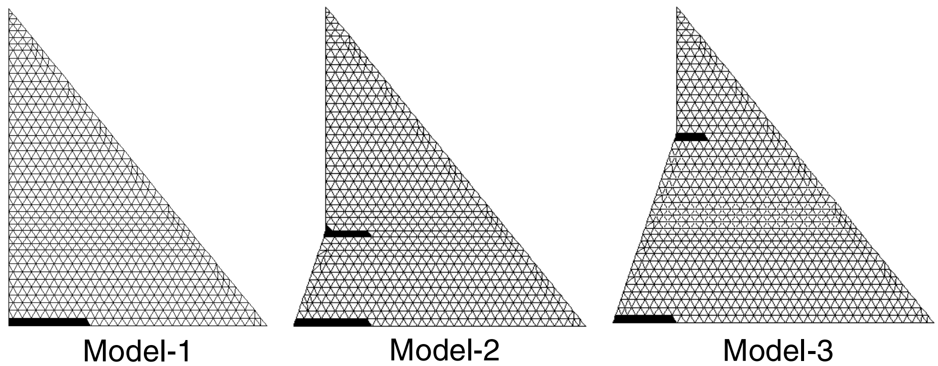

Figure 5 Locations of Final Crack Occurrence

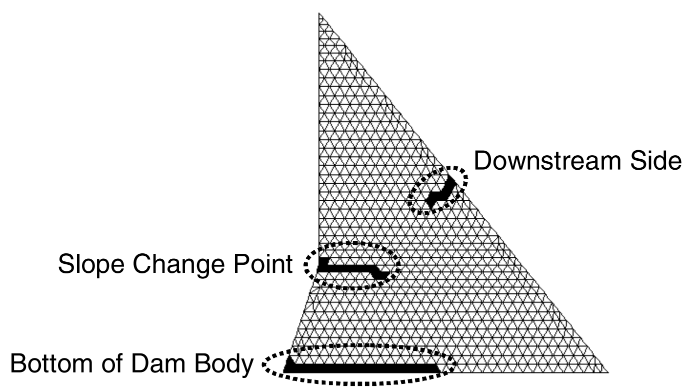

Figure 6 Example of Crack on Downstream

2.2.3 Effect of Stress at Beginning of Tension-Softening

Figure 7 shows the relationship between the stress at the beginning of tension-softening and the crack length (maximum distance from the dam surface to the tip of a crack) in Model-2 on the conditions that the fracture energy is set at the constant value of 300N/m. According to linear analysis results, the dam response became steady up to the fifth wave. Figure 7 (a) shows result for the slope change point and (b) shows that for the bottom of the dam body. From this figure, it is found that with the decrease of the stress at beginning of tension-softening, the crack length becomes longer. It also shows that even when the wave with the same acceleration amplitude is continuously inputted, cracks converge at a certain length without keeping extending. Therefore it is seen that the progress of the crack is small if input does not come at higher level than the input as the crack occurred. In the case of the wave used for this dynamic analysis, the convergent crack length for the fifth wave at the slope change point does not change much by the stress at the beginning of tension-softening.

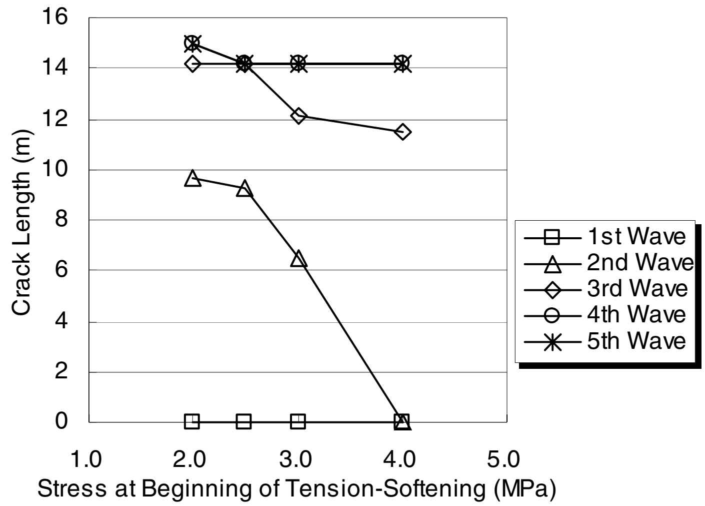

(a) Slope Change Point

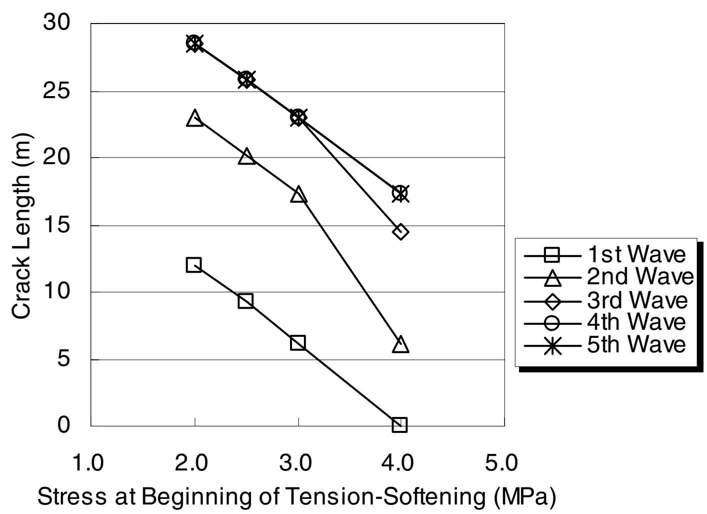

(b) Bottom of Dam Body

Figure 7 Relationship between Crack Length and Stress at Beginning of Tension-Softening (*Gf*=300N/m)

2.2.4 Effect of Fracture Energy

Figure 8 shows the relationship between the crack length and the fracture energy in Model-2 from the first wave to the fifth wave, when the stress at beginning of tension-softening is set at the constant value of 2.5MPa. Figure 8 (a) shows the slope change point and (b) shows the bottom of the dam body. From this figure, it is found that with the increase of the fracture energy, the crack length is shorter and the progress of the crack is prevented further. But there is a point where the crack length increases with the increase of the fracture energy. It is thought that the each crack near the slope change point and the bottom of dam body affect the response of the dam body, and that the above phenomenon is caused as the result of this subtle change. And as the case of the stress at beginning of tension-softening, the progress of the crack is small if input does not come at higher level than the input as the crack occurred, and the crack converges at a certain length.

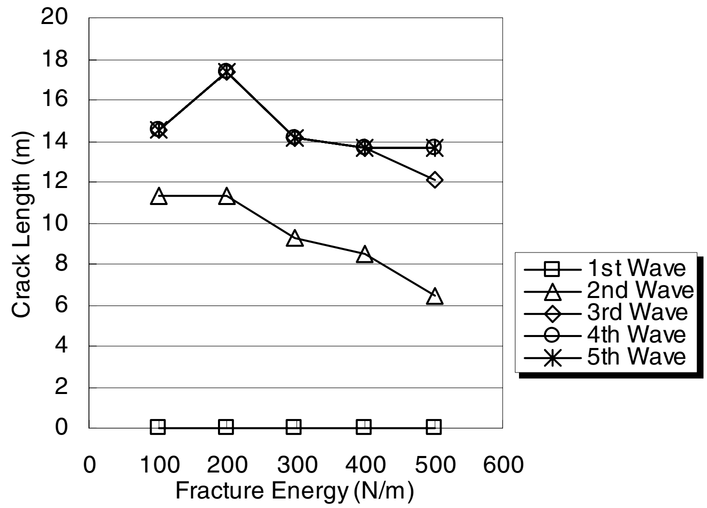

(a) Slope Change Point

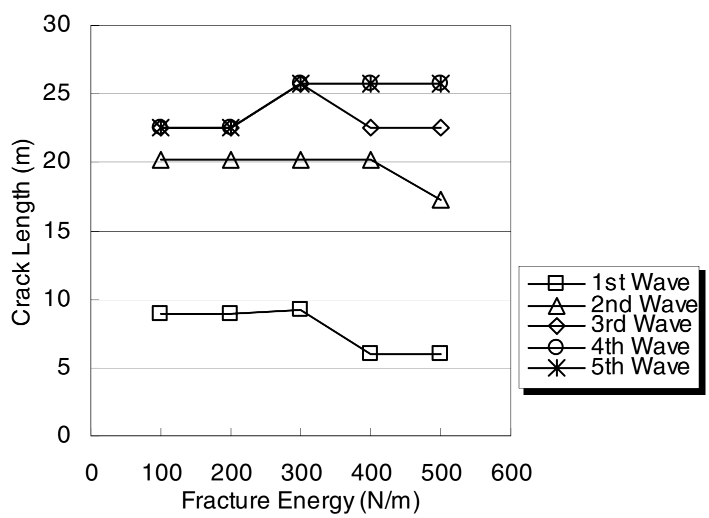

(b) Bottom of Dam Body

Figure 8 Relationship between Crack Length and Fracture Energy (*ft*=2.5MPa)

2.2.5 Comparison of Degree of Effect of Stress at Beginning of Tension-Softening with That of Fracture Energy

Figure 9 shows the relationship between the ratio of the crack length and the ratio of the stress at beginning of tension-softening or of the fracture energy in Model-2. The ratio of the crack length was obtained from a crack length divided by the crack length on condition that the stress at beginning of tension-softening is 2.5MPa and the fracture energy is 300N/m, and standards of the stress at beginning of tension-softening and of the fracture energy are respectively 2.5MPa and 300N/m. The results for the second wave and the fifth wave at the slope change point are shown in Figure 9 (a) and those at the bottom of the dam body are shown in Figure 9 (b). From this figure, it is found that when the crack continues its progress and the response of dam body is not steady as at the second wave, the slope of the trend curve for the stress at beginning of tension-softening is sharper than the fracture energy, so that the effect of the stress at beginning of tension-softening on the crack progress is larger than that of the fracture energy. But when the response of dam body is steady as at the fifth wave, the slopes of the trend curves for the stress at beginning of tension-softening and for the fracture energy are not much sharp and almost equal to zero, and this tendency is more conspicuous at the slope change point than at the bottom of the dam body.

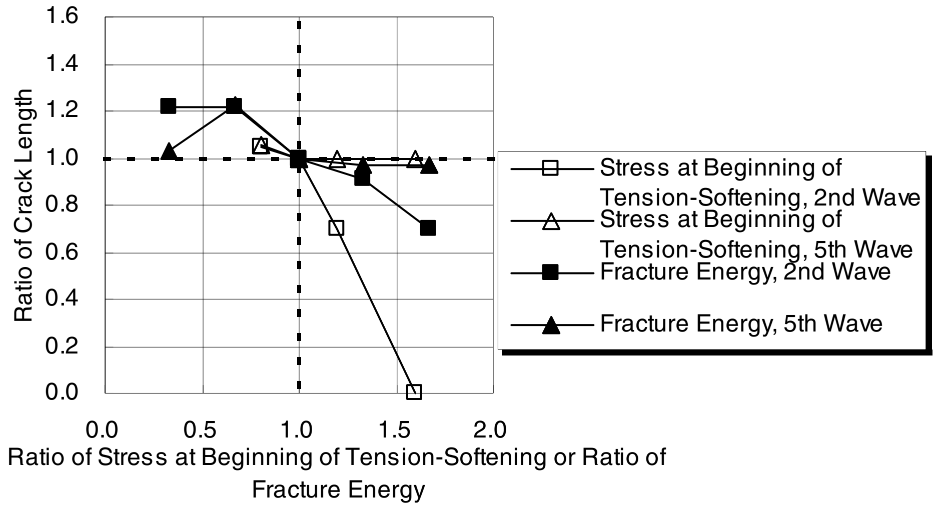

(a) Slope Change Point

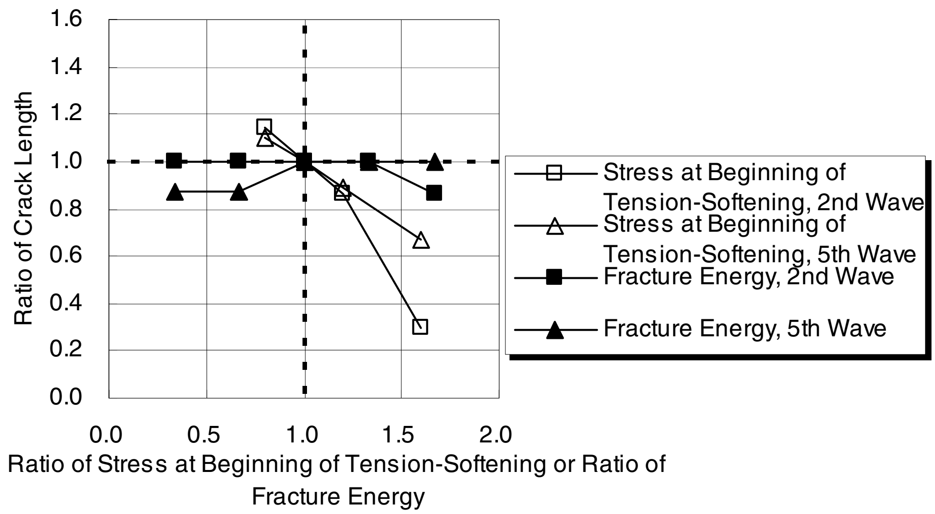

(b) Bottom of Dam Body

Figure 9 Ratio of Crack Length

3. BEHAVIOR UNDER OBSERVED SEISMIC WAVE

3.1 Analysis Conditions

The consideration similar to Chapter 2 was performed using the wave observed at a dam during an earthquake. The analysis model was Model-2 in Figure 1, and the analysis conditions were similar to the above Chapter. As an input wave, we used the acceleration data (max. acceleration of 183gal) observed at the lower inspection gallery of Hitokura Dam during the Kobe Earthquake in 1995. Only the amplitude of the acceleration data was enlarged, and it was inputted in the horizontal direction from the bottom of the dam body with the downstream side as positive. Figure 10 shows the input wave whose maximum acceleration is extended to 300gal.

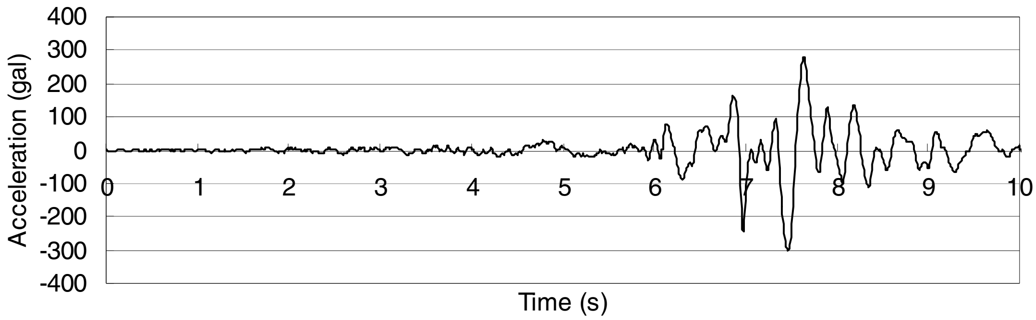

Figure 10 Input Wave (Max. acceleration of 300gal)

3.2 Results of Analysis

3.2.1 Response of Dam Body

Figure 11 shows the time histories of response of acceleration and displacement at the crest obtained by the linear dynamic analysis and the crack progress analysis of Model-2, and Figure 12 shows the location of the final crack by crack progress analysis. The stress at beginning of tension-softening is 2.5MPa and the fracture energy is 300N/m. All cracks shown in Figure 12 occurred at 7.51 seconds when the dam body was the most greatly displaced towards the downstream side. Figure 11 reveals that the later response of the dam body after the occurrence of cracks varied much more than in the case of a linear elastic body.

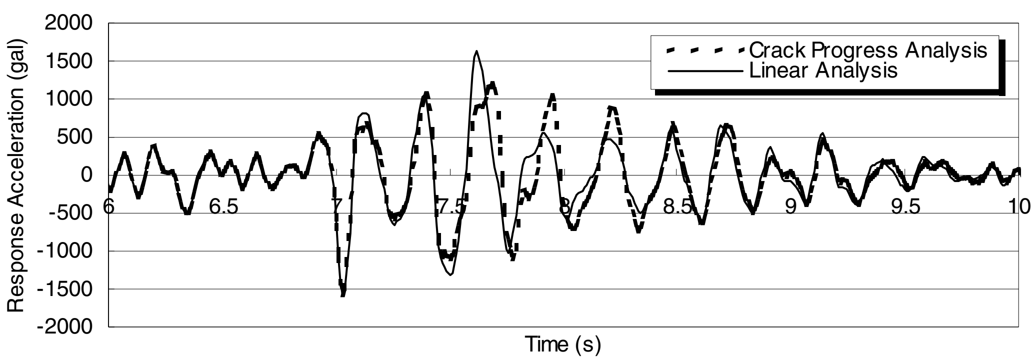

(a) Acceleration

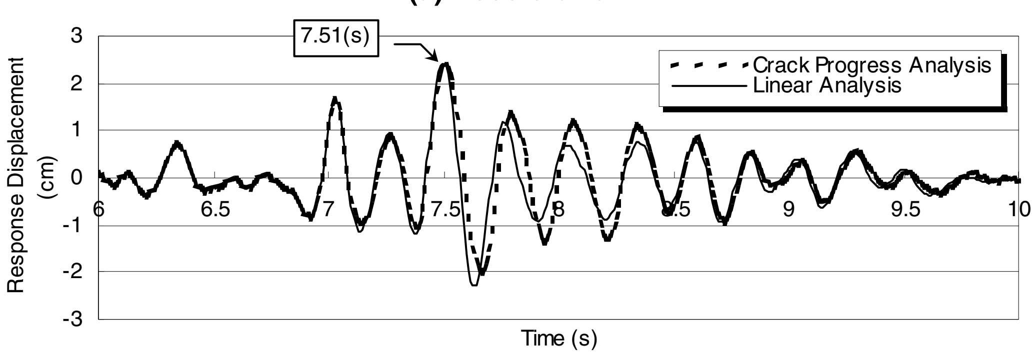

(b) Displacement

Figure 11 Response Time History at Crest of Dam

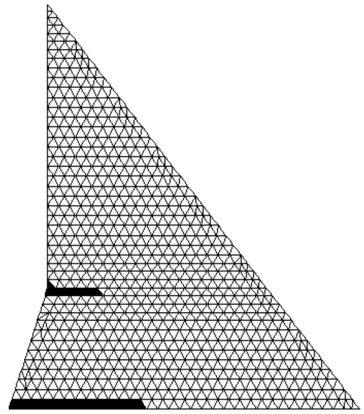

Figure 12 Final Crack Location
(Max. Acceleration 300gal, *ft*=2.5MPa, *Gf*=300N/m)

3.2.2 Effect of Maximum Acceleration on Crack Length

Figure 13 shows the relationship between the crack length and the maximum acceleration at the slope change point and at the bottom of the dam body in Model-2. The stress at beginning of tension-softening is 2.5MPa and the fracture energy is 300N/m. From the figure, it is found that the higher the maximum acceleration is, the longer the crack becomes, and that the maximum acceleration and the crack length have an almost linear relationship.

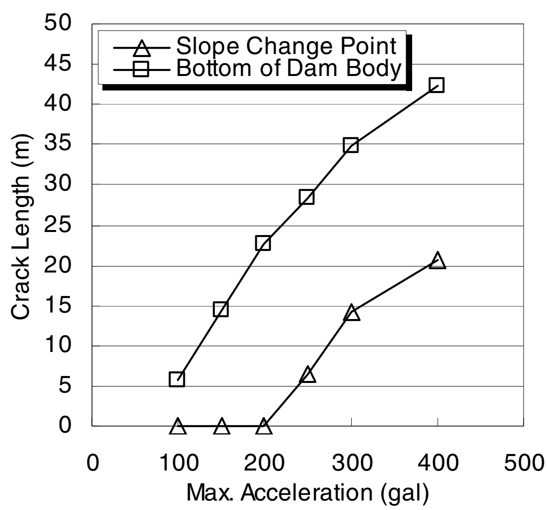

Figure 13 Relationship between Crack Length and Max. Acceleration
(*ft*=2.5MPa, *Gf*=300N/m)

3.2.3 Effect of Stress at Beginning of Tension-Softening on Crack Length

Figure 14 shows the relationship the crack length and the stress at beginning of tension-softening at the slope change point and at the bottom of the dam body in Model-2. The fracture energy is constant at 300N/m. The maximum acceleration of the input wave is fixed at 300gal after this point. From the figure, it is found that the larger the stress at beginning of tension-softening is, the shorter the crack length becomes, and that the stress at beginning of tension-softening and the crack length have an almost linear relationship.

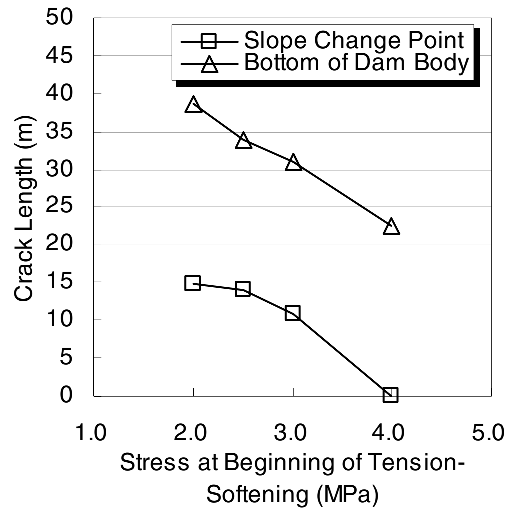

Figure 14 Relationship between Crack Length and Stress at Beginning of Tension-Softening (*Gf*=300N/m)

3.2.4 Effect of Fracture Energy on Crack Length

Figure 15 shows the relationship between the crack length and the fracture energy at the slope change point and at the bottom of the dam body in Model-2. The stress at beginning of tension-softening is a constant value of 2.5MPa. From the figure, it is found that as the fracture energy increases, the crack length tends to decline slightly, but that there is almost no change of crack length at the bottom of the dam body.

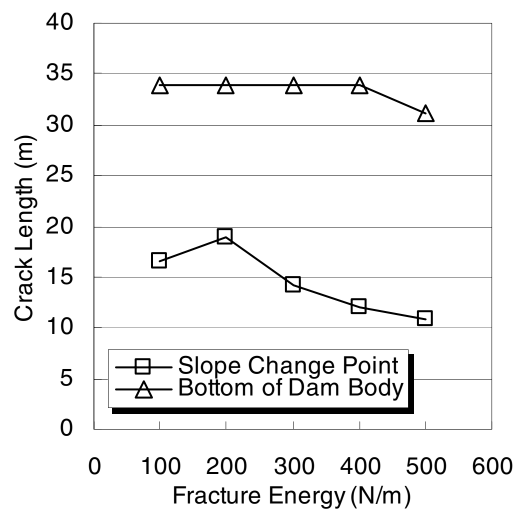

Figure 15 Relationship between Crack Length and Fracture Energy (*ft*=2.5MPa)

3.2.5 Comparison of Degree of Effect of Stress at Beginning of Tension-Softening with That of Fracture Energy

Figure 16 shows the relationship between the ratio of the crack length and the ratio of the stress at beginning of tension-softening or of the fracture energy in Model-2. The ratio of the crack length was obtained from a crack length divided by the crack length on condition that the stress at beginning of tension-softening is 2.5MPa and the fracture energy is 300N/m, and standards of the stress at beginning of tension-softening and of the fracture energy are respectively 2.5MPa and 300N/m. As seen in this figure, it is found that the slope of the trend curve for the stress at beginning of tension-softening is sharper than that for the fracture energy, so that the effect of the stress at beginning of tension-softening on the progress of the crack is greater than that of the fracture energy. This signifies that when material properties used for analysis is set, it is important to estimate the stress at beginning of tension-softening more appropriately than the fracture energy.

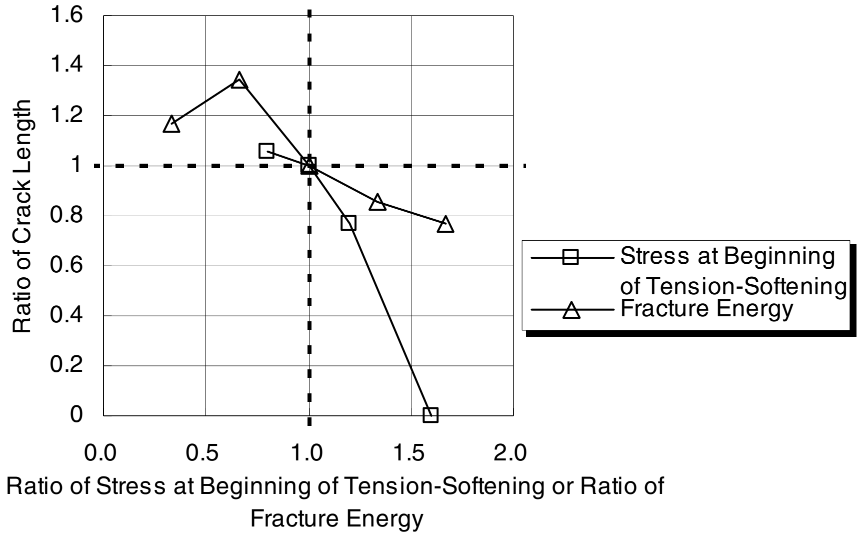

(a) Slope Change Point

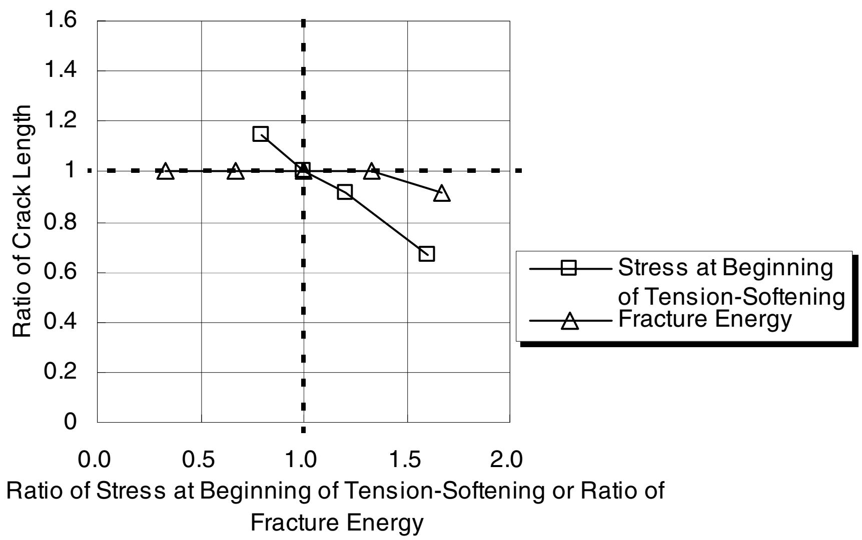

(b) Bottom of Dam Body

Figure 16 Ratio of Crack Length

3.2.6 Comparison with Result for Sinusoidal Wave

Figure 17 shows the relationship between the ratio of the crack length and the ratio of the stress at beginning of tension-softening at the slope change point in Model-2 for the second and fifth sinusoidal wave and the wave observed at the Hitokura Dam, and the crack length on condition of the stress at beginning of tension-softening 2.5MPa and the fracture energy 300N/m is set to the standard. From this figure, it is found that result for the actual seismic wave is considered to be the transitional state than the steady state. The duration of the large acceleration in the Hitokura wave is very short. Therefore, it is possible for crack to progress further if the number of large acceleration waves increases. However, it is thought that though it depends on the type of wave and the maximum acceleration level etc., the progress length of the crack converges at a certain value as the results of the analysis using sinusoidal waves.

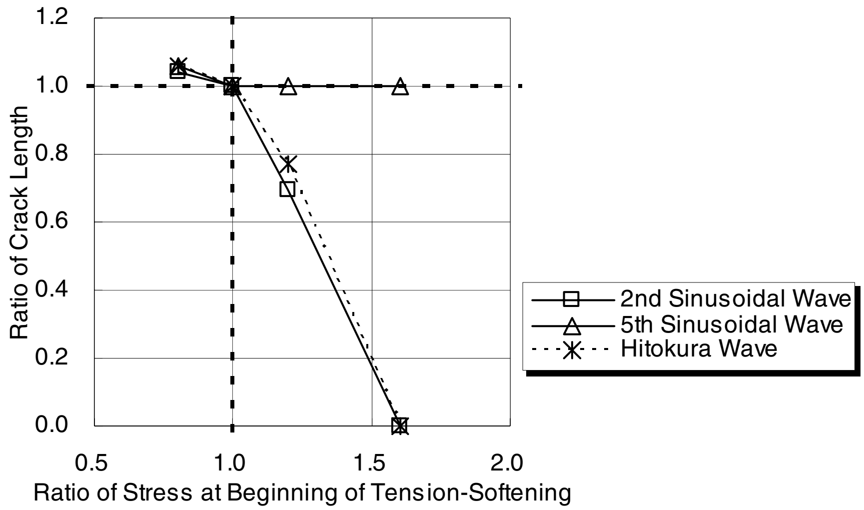

Figure 17 Comparison of Sinusoidal Wave and Observed Seismic Wave

4. CONCLUSIONS

The study of effects of concrete material properties on crack progress was conducted using dynamic analysis with smeared crack model. The followings were found by this study.

(1) Cracks on concrete gravity dams tend to occur at the bottom of the dam body and near the slope change point during earthquakes.
(2) According to the analysis using the sinusoidal waves, crack length converges at a certain length even if waves of acceleration come continuously.
(3) In a state where the crack progress is transitional, the stress at beginning of tension-softening has an effect on the crack length more than the fracture energy.
(4) But in a state where the crack progress is steady, there is little difference between the effect of the fracture energy on the crack length and that of the stress at beginning of tension-softening.
(5) In the case of the analysis using the actual seismic wave with the short duration of the maximum acceleration part, the result shows the transitional state of crack progress than the steady state, and the crack length tends to be affected greatly by the stress at beginning of tension-softening.

REFERENCES

1. Y. Uchida, K. Rokugo and W. Koyanagi: FE-Analysis of Crack Propagation in Plain Concrete Using Smeared Crack Model with Concept of Fictitious Crack Model, Journals of the Japan Society of Civil Engineers, No. 466, Vol. 19, pp. 79-88, May 1993 (in Japanese)
2. H. Zhang and T. Ohmachi: FE-BE Method for Earthquake-induced Cracking of Concrete Gravity Dam-Reservoir Systems, Journal of Japan Society of Dam Engineers Vol. 11, No. 4, pp. 266-274, December 2001 (in Japanese)
3. “DIANA”: general purpose structural analysis software for the civil engineering field, Public Information Journal SENAC, Vol. 32, No. 2, April 1999 (in Japanese)